

Aligned AlN Nanorods with Multi-tipped Surfaces—Growth, Field-Emission, and Cathodoluminescence Properties**

By Jr Hau He, Rusen Yang, Yu Lun Chueh, Li Jen Chou, Lih Juann Chen,* and Zhong Lin Wang*

Aluminum nitride, an important member of the group III nitrides with the highest bandgap of about 6.2 eV, has excellent thermal conductivity, good electrical resistance, low dielectric loss, high piezoelectric response, and ideal thermal expansion, matching that of silicon.^[1] The interest in field-emission (FE) applications of AlN materials has grown because they exhibit a negative electron affinity.^[2] Exhibiting a negative electron affinity means that electrons excited into the conduction band can be freely emitted into vacuum. In addition, high-current emission at a relatively low field is most attractive for FE applications. As a result, significant effort is being devoted to reducing the tip size and increasing the density of the emitting sites by using hierarchical nanostructures. Therefore, the synthesis of AlN nanostructures, such as nanowires,^[3] nanotubes,^[4] nanocones,^[5] nanotips,^[6,7] hierarchical comb-like structures,^[8] and nanobelts,^[9] with controlled high-aspect-ratio shapes and sizes is an important topic worthy of exploration. The promise that one-dimensional (1D) nanostructures may dramatically improve the desired properties for many applications has stimulated great enthusiasm. For example, FE properties of various AlN nanostructures have been investigated. The turn-on fields of various 1D aluminum nitride nanostructures have been measured, such as nanowires ($8.8 \text{ V } \mu\text{m}^{-1}$),^[3] nanocones ($12 \text{ V } \mu\text{m}^{-1}$),^[5] nanotips ($3.1\text{--}4.7 \text{ V } \mu\text{m}^{-1}$),^[6,7] and hierarchical comb-like structures ($2.45\text{--}3.76 \text{ V } \mu\text{m}^{-1}$).^[8] On the other hand, reports on the luminescence properties of AlN nanostructures are scarce.^[9] The AlN nanocones have been observed to have an emission band centered at 481 nm, referred to as a deep-level or trap-level state.^[5]

In the present study, we report the growth of well-aligned AlN nanorods with hairy surfaces by a vapor–solid (VS) process. The well-aligned AlN nanorods with hairy surfaces reported here not only provide a new hierarchical nanostructure,

but also serve as a promising candidate for FE emitters because of their low electron affinity and the geometry of the multiple-nanotip surfaces. Compared with previous reports on hierarchical growth of AlN nanostructures,^[8,10] in this communication we report a higher density of smaller nanotips ($\sim 3\text{--}15 \text{ nm}$) that were radially grown on the surfaces of AlN nanorods. Each nanotip may serve as an ultrasmall emitter. In addition, growing well-aligned AlN nanorods on Si substrates is amenable to current technology for the fabrication of Si-based microelectronics devices. The subsequent characterization of their cathodoluminescence (CL) reveals that these hierarchical AlN nanostructures possess an intense emission peak, further suggesting potential applications in optoelectronic nanodevices.

The structure of the as-grown products has been determined by X-ray diffraction (XRD). As shown in Figure 1, all of the diffraction peaks in the XRD pattern can be identified; they correspond to a hexagonal wurtzite-structured AlN crystal

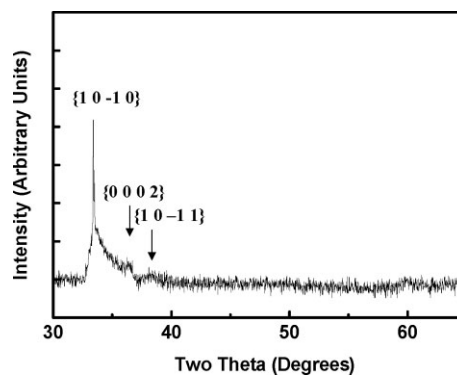


Figure 1. XRD pattern of the as-synthesized products.

tal with lattice constants of $a = 0.3114 \text{ nm}$ and $c = 0.4986 \text{ nm}$, consistent with the Joint Committee Powder Diffraction Standard (JCPDS) data file (Card No. 08-0262). No other impurity phases were found in the XRD pattern.

The morphology of the as-synthesized products has been characterized by scanning electron microscopy (SEM). As shown in Figure 2a, a typical low-magnification SEM image indicates that the as-synthesized product consists of a large quantity of uniform nanostructures. A representative cross-sectional SEM image (Fig. 2b) reveals that AlN nanorods grew vertically from the substrate to form arrays with high density. These well-aligned, columnar AlN nanorods have diameters of about 200–400 nm and lengths of up to $\sim 3.4 \mu\text{m}$,

[*] Prof. Z. L. Wang, J. H. He, R. S. Yang
School of Materials Science and Engineering
Georgia Institute of Technology
Atlanta, GA 30332-0245 (USA)
E-mail: zhong.wang@mse.gatech.edu

Prof. L. J. Chen, J. H. He, Y. L. Chueh, L. J. Chou
Department of Materials Science and Engineering
National Tsing Hua University
Hsinchu 300 (Taiwan)
E-mail: ljchen@mx.nthu.edu.tw

[**] The research was supported by NSF, DARPA, NASA, and NSC, Taiwan. The authors thank Dr. Yong Ding for his kind help in the EELS experiments.

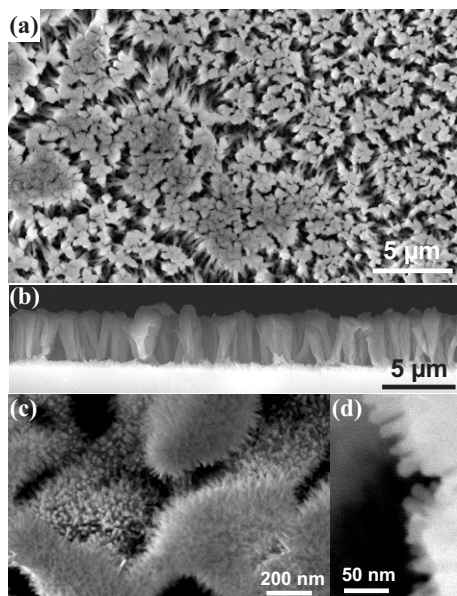


Figure 2. Typical SEM images of the morphologies of the as-synthesized AlN product. a) Low-magnification plan-view image; b) low-magnification cross-sectional image; c) medium-magnification image of AlN nanorods with multiple-nanotip surfaces; d) high-magnification image of the surface of an AlN nanorod.

resulting in an aspect ratio as high as 17. Figure 2c shows the morphologies of AlN nanostructures in more detail. On each columnar nanorod, there are a number of uniform crystallites radially oriented along the main trunk. From the high-magnification SEM images shown in Figure 2d, it is observed that each columnar nanorod is composed of high-density AlN nanotips grown radially along the main trunk. The length and diameter of the numerous AlN nanotips on a columnar trunk of AlN are about ~ 35 nm and $\sim 3\text{--}15$ nm, respectively, resulting in average aspect ratios of $\sim 2.3\text{--}11.6$.

The AlN nanostructures have been further characterized by transmission electron microscopy (TEM) and high-resolution TEM (HRTEM). Figures 3a,b show bright-field and dark-field TEM images of two nanorods, revealing that each columnar nanostructure consists of a main trunk (nanorod core) and packed secondary branches (nanotips). The nanorod cores extend throughout the entire length, whereas the nanotips grow on the surface of the nanorod cores in the radial direction. Each nanorod is composed of tiny nanocrystallites of AlN. The bright dots in the dark-field TEM images (Figs. 3b,c) correspond to the nanocrystallites, which have diameters of 3–15 nm. Selected-area electron diffraction (SAED) was utilized to investigate the phase of the synthesized nanostructures. The rings recorded in the diffraction pattern correspond to the wurtzite AlN crystal, as shown in Figure 3d. Quantifying the nitrogen content is essential to identify the existence of AlN. Electron energy-loss spectroscopy (EELS) measurements have been made to analyze the composition of the synthesized nanorods. Since EELS has a high sensitivity to light elements, it is well suited for chemical analysis of AlN structures. It is known that the energy-loss near-edge structure

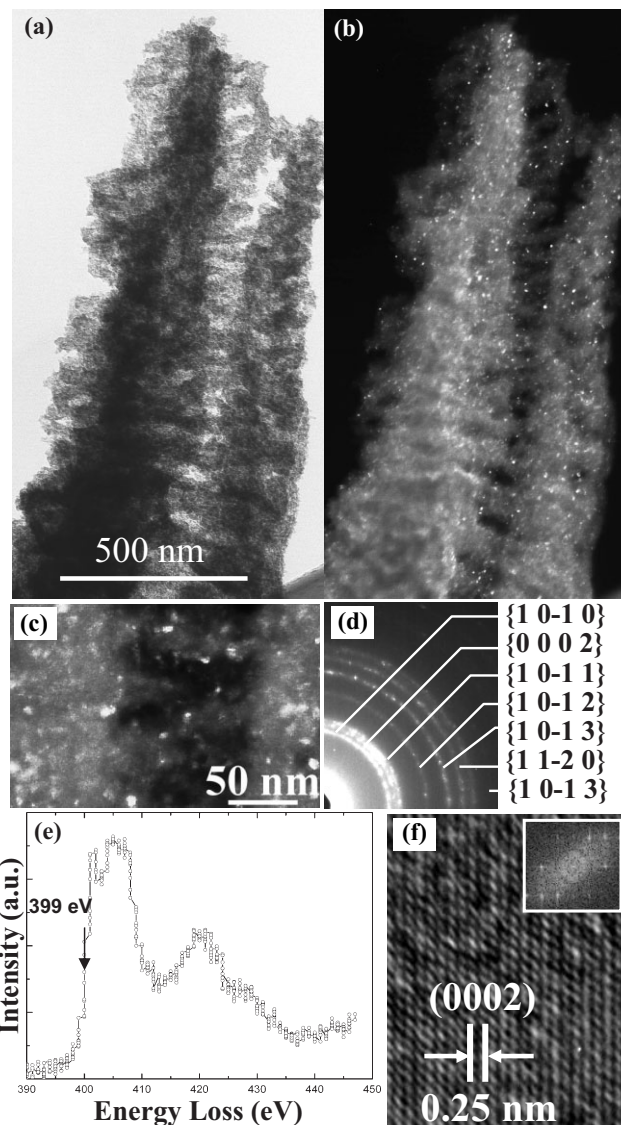


Figure 3. Characterization of the AlN nanostructures. a) Bright-field and b) dark-field TEM images of two columnar AlN nanorods; c) enlarged dark-field TEM image showing the AlN nanocrystallites, 3–5 nm in diameter; d) selected-area electron diffraction pattern of the nanorod, displaying a polycrystalline structure of each rod; e) nitrogen K-edge energy-loss near-edge structure recorded from the sample; f) HRTEM image of a single nanotip. The inset shows a fast-Fourier-transform pattern.

(ELNES) of an EELS spectrum represents a “fingerprint” of the local electronic structure, i.e., the observed ELNES provides information concerning the structure and chemical properties of the atoms that have undergone excitation. Figure 3e shows a representative EELS spectrum after subtraction of the background, showing nitrogen K-edge ELNES. The shape of the ELNES from the nitrogen K-edge is very similar to that of unoxidized AlN thin films.^[11] No doubt nitrogen is one of the primary elements in the as-synthesized nanostructures. Figure 3f shows an HRTEM image of the nanotip growing along [0001]. The inset to Figure 3f shows a fast Fourier transform (FFT) of the image.

In most cases, the AlN nanotips grew on the surface of columnar AlN nanorods. However, they also grew on the surface of wetting layers (or the bottom of AlN columnar nanorods), forming an entirely nanotip-covered structure (Fig. 4). This corresponds to the morphology of nanostructures grown by the VS mechanism.

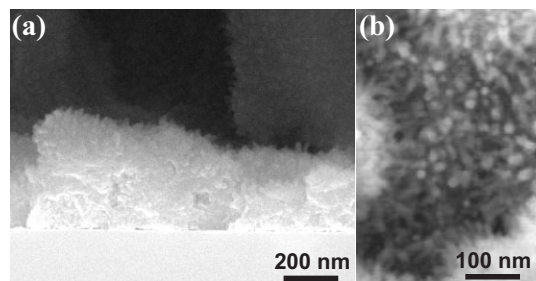
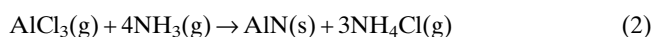


Figure 4. Typical high-magnification SEM images of wetting layers of AlN nanostructures: a) cross-sectional image; b) plan-view image.

We now examine the chemical process for forming AlN. AlCl_3 and $(\text{NH}_4)_2\text{CO}_3$ have been used as aluminum and nitrogen sources, respectively. The sublimation temperature of AlCl_3 is 180°C . $(\text{NH}_4)_2\text{CO}_3$, on exposure to air or heating, undergoes decomposition as



with liberation of ammonia. The boiling point of NH_3 is -33°C . Because of the low sublimation temperature of AlCl_3 and the low boiling point of NH_3 , AlN has been observed to form even at 600°C or lower via the gas-phase reaction of AlCl_3 and NH_3 .^[11,12]



Based on our observations, a possible mechanism for the formation of the hierarchical AlN nanostructures is likely to consist of the following consecutive steps: 1) As the processing temperature increases, thermal decomposition of AlCl_3 and $(\text{NH}_4)_2\text{CO}_3$ powders results in the formation of Al and N vapors. The ultrathin films of Ni catalyst provide an energetically favored site for the absorption of incoming AlN vapor (or clusters), resulting in the formation of a solid-solution compound, i.e., heterogeneous growth. With the continuing adsorption of AlN vapors, the solid-solution compound becomes supersaturated. The AlN compound will then precipitate from the solution, yielding the 1D AlN nuclei at the interface between the substrate and the supersaturated compound solution, resulting in continuing growth of 1D columnar AlN nanorods. In addition, no compounds were found to deposit on the Si substrate without the presence of a Ni catalyst. Therefore, the Ni catalyst is critical for growing the well-aligned AlN nanorods in the present study. Similarly, in a previous study,^[5] cone-like AlN arrays have been found to

grow in the reaction between AlCl_3 and NH_3 catalyzed by a Ni thin film. 2) The columnar AlN nanorods can also be used as templates for the adsorption of the AlN vapors during the process, resulting in the formation of AlN nuclei on the side surfaces of growing AlN columnar nanorods. The AlN nanotips can grow on the columnar AlN nanorods with a continuous supply of AlN vapor, i.e., the hairy structure is formed by a homogeneous growth process. Finally, the AlN hierarchical nanostructures were obtained. In a previous study, secondary AlN nanorods grown on the stems of AlN nanorods/nanobelts via condensation of AlN vapor were also observed.^[10]

Nanorods are ideal objects for electron FE. Figure 5 shows the FE current density as a function of the applied field as a current density versus electric field (J - E) plot, and the inset shows a $\ln(J/E^2) - 1/E$ plot of the AlN nanostructures. The

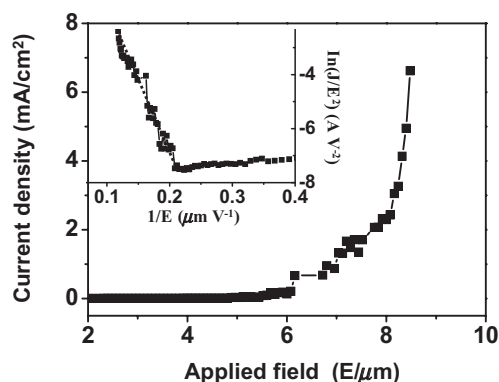


Figure 5. Field-emission current density versus electric field (J - E) for hierarchical AlN nanostructures. The inset shows the corresponding Fowler–Nordheim relationship ($\ln(J/E^2) - 1/E$ plot).

well-aligned columnar AlN nanorods with multiple-nanotip surfaces have excellent turn-on-field values. The turn-on field (defined to be the electric field required to generate a current density of 0.01 mA cm^{-2}) and threshold field (defined to be the electric field required to generate a current density of 1 mA cm^{-2}) for the AlN nanostructures were found to be about 3.8 and $7 \text{ V } \mu\text{m}^{-1}$, respectively. Although the value of the turn-on field from the AlN nanostructure on a sapphire substrate is higher than the best value found for carbon nanotubes^[13] and SiC,^[14] they are much lower than those of many other types of emitters such as carbon nitride,^[15] Si nanostructures,^[16] MoO_3 nanobelts,^[17] and ZnO nanowires.^[18] In a previous study, the selection of the substrate was found to be critical to the FE properties of AlN nanostructures.^[19] Si has been selected as the substrate in the present study since it is more compatible with the processing technology of Si-based microelectronic devices.

Based on the Fowler–Nordheim (FN) model, the FE current from a metal or semiconductor is attributed to the tunneling of electrons through the potential barrier from the material into vacuum under the influence of an electric

field.^[20] In order to understand the FE behavior, the J - E data have also been analyzed by applying the FN equation

$$J = (A\beta^2 E^2 / \Phi) \exp[-B\Phi^{3/2} (\beta E)^{-1}] \quad (3)$$

where J is the current density, E is the applied electric field, and Φ is the work function. A and B are constants, corresponding to $1.56 \times 10^{-10} \text{ A eV V}^{-2}$ and $6.83 \times 10^3 \text{ eV}^{-3/2} \mu\text{m}^{-1}$, respectively. The FN plot is shown in the inset to Figure 5. By determining the slope of the $\ln(J/E^2) - 1/E$ plot using the work-function value of AlN (3.7 eV), the field-enhancement factor, β , has been calculated to be about 950 for well-aligned, columnar AlN nanorods with multiple nanotip surfaces. The β -value is highly dependent on the geometrical features of the nanostructures.^[21] Efficient electron emission from well-aligned, columnar AlN nanorods has mainly been attributed to the small radii of curvature of their multiple-nanotip surfaces, resulting in a high β -value.

Figure 6 shows the room-temperature cathodoluminescence (CL) emission spectrum, demonstrating a broad emission ranging from 350 to 700 nm with a peak at about 519 nm

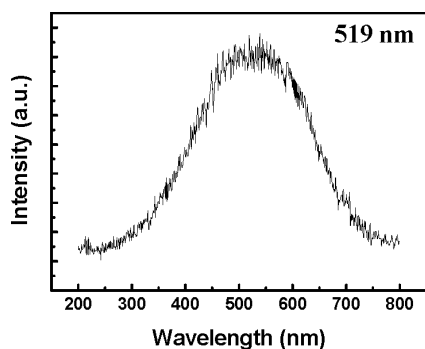


Figure 6. The room-temperature CL emission spectrum of hierarchical AlN nanostructures.

in the yellow-light range. Obviously, the emission does not result from band-edge emission, but is referred to as deep-level or trap-level emission. Specifically, the intensive light emission from AlN materials has generally been attributed to the nitrogen deficiency and the radiative recombination of a photon- (or electron-) generated hole with an electron occupying the nitrogen deficiency;^[5] this phenomenon has also been observed previously in AlN thin-film and nanodot structures.^[22,23] The intensive CL emission indicates that well-aligned, columnar AlN nanorods with multiple-nanotip surfaces have potential application in light-emitting nanodevices.

In summary, this study presents a method for growing well-aligned, columnar AlN nanorods with multiple-nanotip surfaces via the reaction of AlCl_3 and $(\text{NH}_4)_2\text{CO}_3$ by a VS process. The overall nanostructure has an aligned columnar structure, and each nanorod has a hairy surface. As a result, excellent FE properties have been obtained. FE measurements showed that the synthesized AlN nanostructures

have a low turn-on field of $3.8 \text{ V } \mu\text{m}^{-1}$. Intensive light emission from AlN materials has been observed. With excellent FE and CL properties, the novel hierarchical AlN nanostructures have potential applications in optoelectronic and FE nanodevices.

Experimental

Single-crystalline, 3–5 Ωcm , phosphorous-doped Si(001) wafers were used in the present study. The silicon wafers were cleaned chemically by the standard RCA cleaning process. The wafers were dipped in a dilute HF solution ($\text{HF}/\text{H}_2\text{O} = 1:50$) for 2 min immediately before loading into a thermal-evaporation system. An ultrathin Ni film (3 nm thick) was deposited at $\sim 2 \times 10^{-5}$ torr (1 torr \sim 133 Pa) onto a Si substrate at room temperature by thermal evaporation at the rate of 0.1 nm s^{-1} . This Ni thin film served as the catalyst for heterogeneous growth of the AlN nanostructures. The processes were usually carried out in a horizontal tube furnace, which is composed of a horizontal quartz-tube furnace, an alumina tube, a rotary-pump system, and a gas supply and control system. A viewing window was set up at the end of the alumina tube and was used to monitor the growth process. The opposite end of the tube was connected to the rotary pump. Both ends were sealed by rubber O-rings. The ultimate vacuum for this configuration was $\sim 2 \times 10^{-3}$ torr. AlCl_3 and $(\text{NH}_4)_2\text{CO}_3$ were used as aluminum and nitrogen sources, respectively. 0.004 mol of AlCl_3 powder was placed at the center of the horizontal alumina-tube furnace, where the temperature was the highest. 0.004 mol of $(\text{NH}_4)_2\text{CO}_3$ powder was positioned at the front part of the horizontal alumina-tube furnace upstream of AlCl_3 . The substrates were placed in a lower temperature zone, downstream from AlCl_3 . In a typical run, after being evacuated to a pressure of $\sim 2 \times 10^{-3}$ torr, the furnace was heated from room temperature to 1000°C at a heating rate of $60^\circ\text{C min}^{-1}$ under H_2 flow at 25 sccm (standard cubic centimeters per minute). The samples were held at 1000°C for 30 min, and the chamber pressure was kept at 90 torr.

After the growth process, the product was identified by XRD (Philips PW 1800 with $\text{Cu K}\alpha$ radiation). The substrate-bound nanorods were mechanically scraped off, sonicated in ethanol, and deposited on carbon-coated copper grids for TEM characterization. Morphological studies of grown AlN nanostructures were performed with a JEOL 4000EX TEM with a point-to-point resolution of 0.18 nm, operating at 400 kV, and with a JEOL JSM-6500 FE SEM.

The CL spectrum was measured in a scanning electron microscope with an electron-probe microanalyzer (Shimadzu EPMA-1500). CL spectra were accumulated in the single-shot mode in 1 s. The FE measurements of the AlN nanostructures were carried out at a vacuum of 1×10^{-7} torr using a spherical stainless-steel probe (1 mm in diameter) as the anode. The emission current was recorded on the level of nanoamperes. The distance between the anode and the emitting sample's (cathode) surface was fixed at 50 μm .

Received: August 28, 2005

Final version: December 6, 2005

- [1] S. M. Bradshaw, J. L. Spicer, *J. Am. Ceram. Soc.* **1999**, *82*, 2293.
- [2] M. C. Benjamin, C. Wang, R. F. Davis, R. J. Nemanich, *Appl. Phys. Lett.* **1994**, *64*, 3288.
- [3] Y. B. Tang, H. T. Cong, Z. G. Zhao, H. M. Cheng, *Appl. Phys. Lett.* **2005**, *86*, 153 104.
- [4] Q. Wu, Z. Hu, X. Z. Wang, Y. N. Lu, X. Chen, H. Xu, Y. Chen, *J. Am. Chem. Soc.* **2003**, *125*, 10 176.

- [5] C. Liu, Z. Hu, Q. Wu, X. Z. Wang, Y. Chen, H. Sang, J. M. Zhu, S. Z. Deng, N. S. Xu, *J. Am. Chem. Soc.* **2005**, *127*, 1318.
- [6] S. C. Shi, C. F. Chen, S. Chattopadhyay, Z. H. Lan, K. H. Chen, L. C. Chen, *Adv. Funct. Mater.* **2005**, *15*, 781.
- [7] Q. Zhao, J. Xu, X. Y. Xu, Z. Wang, D. P. Yu, *Appl. Phys. Lett.* **2004**, *85*, 5331.
- [8] L. W. Yin, Y. Bando, Y. C. Zhu, M. S. Li, Y. B. Li, D. Golberg, *Adv. Mater.* **2005**, *17*, 110.
- [9] K. J. Lee, D. H. Ahn, Y. S. Kim, *J. Am. Ceram. Soc.* **2000**, *83*, 1117.
- [10] Q. Wu, Z. Hu, X. Z. Wang, Y. Chen, Y. Lu, *J. Phys. Chem. B* **2003**, *107*, 9726.
- [11] M. MacKenzie, A. J. Craven, *J. Phys. D: Appl. Phys.* **2000**, *33*, 1647.
- [12] M. C. Wang, M. S. Tsai, N. C. Wu, *J. Cryst. Growth* **2000**, *210*, 487.
- [13] A. M. Rao, D. Jacques, R. C. Haddon, W. Zhu, C. Bower, S. Jin, *Appl. Phys. Lett.* **2000**, *76*, 3813.
- [14] Z. W. Pan, H. L. Lai, F. C. K. Au, X. F. Duan, W. Y. Zhou, W. S. Shi, N. Wang, C. S. Lee, N. B. Wong, S. T. Lee, S. S. Xie, *Adv. Mater.* **2000**, *12*, 1186.
- [15] E. J. Chi, J. Y. Shim, H. K. Baik, S. M. Lee, *Appl. Phys. Lett.* **1997**, *71*, 324.
- [16] T. Sugino, S. Kawasaki, K. Tanioka, J. Shirafuji, *Appl. Phys. Lett.* **1997**, *71*, 2704.
- [17] Y. B. Li, Y. Bando, D. Golberg, K. Kurashima, *Appl. Phys. Lett.* **2002**, *81*, 5048.
- [18] Y. K. Tseng, C. J. Huang, H. M. Cheng, I. N. Lin, K. S. Liu, I. C. Chen, *Adv. Funct. Mater.* **2003**, *13*, 811.
- [19] S. C. Shi, C. F. Chen, S. Chattopadhyay, K. H. Chen, L. C. Chen, *Appl. Phys. Lett.* **2005**, *87*, 73109.
- [20] R. H. Fowler, L. W. Nordheim, *Proc. R. Soc. London, Ser. A* **1928**, *119*, 173.
- [21] R. S. Chen, Y. S. Huang, K. H. Lee, Y. Jeong, *Appl. Phys. Lett.* **2004**, *78*, 2052.
- [22] J. Li, K. B. Nam, M. L. Nakarmi, J. Y. Lin, H. X. Jiang, *Appl. Phys. Lett.* **2002**, *81*, 3365.
- [23] Y. C. Lan, X. L. Chen, Y. G. Cao, Y. P. Xu, L. D. Xun, T. Xu, J. K. Liang, *J. Cryst. Growth* **1999**, *207*, 247.